The dual-channel logic controller synthesis for controlling complex dynamic objects

Victoria Vysotska[1,†], Serhii Vladov[2,*,†], Oleksandr Lavrut[3,†], Oleksandr Muzychuk[4,†] and Denys Baranovskyi[5,†]

[1] *Lviv Polytechnic National University, Stepan Bandera Street 12 79013 Lviv, Ukraine*

[2] *Kremenchuk Flight College of Kharkiv National University of Internal Affairs, Peremohy Street 17/6 39605 Kremenchuk, Ukraine*

[3] *Hetman Petro Sahaidachnyi National Army Academy, Heroes of Maidan 32 79026 Lviv, Ukraine*

[4] *Kharkiv National University of Internal Affairs, L. Landau Avenue 27 61080 Kharkiv, Ukraine*

[5] *Rzeszow University of Technology, Kwiatkowskiego Street 4 37-450 Stalowa Wola, Poland*

Abstract
This research evaluates the helicopter turboshaft engines proposed dual-channel logic controller, demonstrating its effectiveness in controlling complex dynamic systems under parametric uncertainty. A structure and functioning algorithm for a dual-channel logic controller is proposed, accounting for both the dynamics of each separate subsystem and their mutual influence when generating the control action. The research assesses this controller using the TV3-117 engine across various flight parameters, including bench test conditions (H = 0 km, V = 0 Mach) and two flight scenarios (H = 2.5 km, V = 0.68 Mach; H = 4.2 km, V = 0.86 Mach). Results reveal that the controller reduces error from 2.58 to below 1 %, reflecting nearly a 40 % improvement in performance. Despite these gains, the research notes limitations: the controller's effectiveness is based on a specific engine model and may not generalize to other engines or more complex conditions. Additional research is necessary to explore its robustness and adaptability to a broader range of operational scenarios and engine types.

Keywords
dual-channel logic controller, helicopter turboshaft engines, controlling, subsystems, multi-connected automatic control system (MCACS)

1. Introduction

Modern complex dynamic systems (CDS), such as helicopter turboshaft engines (TE), consist of several interconnected subsystems that interact through natural cross-links within the object [1]. These interactions significantly complicate the control process, requiring the internal structure and dynamic relations deep understanding between system elements for effective control [2].

Helicopter TE, as multi-dimensional control objects, are characterized by nonlinear system elements and non-stationary processes, leading to significant changes in parameters under different operating conditions [3]. The dynamic and static characteristics of such objects vary depending on operating modes, demanding adaptive approaches in designing automatic control systems (ACS) [4]. A particular challenge is the need to account for the cross-links impact between subsystems on the overall system's output parameters [5].

An essential task is the control algorithms development that ensure the multi-connected system effective operation across all operating modes. Traditional linear design methods for multi-

connected ACS in helicopter TE do not fully address the challenges related to achieving the required tactical and technical performance [5, 6]. Therefore, more flexible and adaptive approaches to control are necessary to guarantee the reliability and efficiency of these complex dynamic systems.

2. Related works

The CDS control issue, including helicopter TE, is extensively discussed in the literature. Several researches emphasize that such systems are characterized by significant nonlinearity and variable parameters depending on operating modes, which complicates the traditional methods application for designing ACS [7, 8]. Researchers highlight the necessity of considering non-stationary processes and intricate interactions between subsystems when developing multi-connected ACS, particularly in aviation contexts [9–11].

Other researchers focus on the linear control methods limitations, which often fail to provide sufficient accuracy and reliability in multi-dimensional systems controlling like helicopter TE. The researchers [12–14] underline the need for nonlinear adaptive algorithms that account for the systems dynamic behavior in real time. These approaches enable better adaptation to changing operating conditions, improving the overall reliability and safety of the system.

The most attention in modern literature is directed towards developing new methods for synthesizing multi-connected control systems that ensure stability and precision under various operating conditions [15, 16]. Specifically, algorithms incorporating neural networks and machine learning techniques have been proposed to predict system behavior and adjust control parameters in real time [17–19]. These innovative methods significantly enhance the ACS efficiency and help achieve the tactical and technical performance required in aviation technology.

Despite significant advances in complex dynamic systems controlling, such as helicopter TE, several unresolved issues remain related to ensuring the ACS accuracy and reliability in conditions with multiple dimensions and changing parameters. Current research does not sufficiently consider the cross-links impact between subsystems, which reduces the control effectiveness when operating modes change. Additionally, linear and traditional adaptive control methods are not always adequately capable responding to nonlinear processes and rapid transient modes, creating a need for the multi-channel logic controller development. Such a controller could provide more accurate real-time adjustments to control parameters, accounting for system interconnectivity and enhancing the ACS stability and adaptability across an operating conditions wide range.

3. Materials and methods

In researchers [20–22], the helicopter TE properties as multi-connected control systems are explored. The helicopter TE is described as stable, non-stationary systems, whose dynamic parameters shift with changes in external flight conditions. The helicopter TE nonlinear dynamic model is complex, making the multi-connected automatic control systems (MCACS) synthesis and analysis challenging. To simplify this process, the model is typically represented by a system of linearized stationary differential equations [23, 24]. In this article, the helicopter TE (using the TV3-117 engine from the Mi-8MTV helicopter as an example [25, 26]) is presented as a multi-connected control system with three regulated coordinates, which are the engine functional parameters: the gas-generator rotor r.p.m. (n_{TC}), the free turbine rotor speed (n_{FT}), and the gas temperature before the compressor turbine (T_G^*) [27]. The control input is the fuel consumption into the combustion chamber (G_T). Based on this, the helicopter TE matrix transfer function (MTF), along with its actuator, is represented as follows [28]:

$$W_{TE}(s) = \frac{1}{(T_{act} \cdot s + 1) \cdot (T_{eng} \cdot s + 1)} \times \qquad (1)$$

$$\times \begin{pmatrix} K_{11} & K_{12} & -K_{13} \\ K_{21} \cdot (\tau_{21} \cdot s + 1) & K_{22} \cdot (\tau_{22} \cdot s + 1) & -K_{23} \cdot (\tau_{23} \cdot s + 1) \\ K_{31} \cdot (\tau_{31} \cdot s + 1) & -K_{32} \cdot (\tau_{32} \cdot s + 1) & K_{33} \cdot (\tau_{33} \cdot s + 1) \end{pmatrix},$$

where T_{act} is the actuator time constant, T_{eng} is the engine time constant, τ_{ij} are the subsystem forcing time constants, K_{ij} are the gain coefficients.

The helicopter TE MTF parameters are determined by flight parameters. There are altitude (H, km) and speed (V, M), where M is the Mach number. Since altitude and speed vary significantly during flight, the helicopter TE parameters also fluctuate considerably [29]. A linear approach to MCACS designing [30] will not provide the required control quality for helicopter TE. This underscores the need to develop new control algorithms that effectively utilize all available resources to meet the technical requirements across all operating modes. Based on [31, 32], this research proposes using logic controllers within the helicopter TE MCACS separate subsystems to address this issue.

A promising approach for synthesizing helicopter TE MCACS is the logic controllers use that adjust both the control device's structure and parameters based on their operational logic. These logic controllers greatly enhance the ability to direct control processes, thereby improving the entire system dynamic and static properties [33]. Consider the helicopter TE MCACS [34], which includes logic controllers within its separate subsystems. The structural diagram is shown in Figure 1, where $\mathbf{G}(t)$, $\mathbf{U}(t)$, and $\mathbf{Y}(t)$ represent the vectors for reference, control, and regulated coordinates, respectively, and $\boldsymbol{\varepsilon}(t)$ denotes the control errors vector.
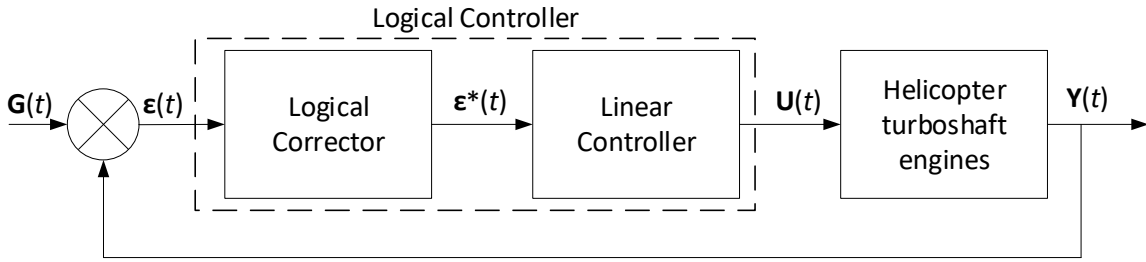
Figure 1: The helicopter turboshaft engines multi-connected automatic control system with a logical controller structural diagram.

A key challenge in using logic controllers is developing an algorithm that incorporates the controlled object structural and parametric characteristics when generating control actions, while also establishing a straightforward relation between the system's coordinates and the required control signals. Numerous logical control laws exist, such as those described in [35–37]:

$$\varepsilon^*(t) = \begin{cases} k_1 \cdot \varepsilon(t) \ at \ \varepsilon'(t) \cdot \varepsilon''(t) > 0 \\ k_2 \cdot \varepsilon(t) \ at \ \varepsilon'(t) \cdot \varepsilon''(t) < 0 \end{cases} \tag{2}$$

$$\varepsilon^*(t) = \begin{cases} k_1 \cdot \varepsilon(t) \ at \ (T \cdot \varepsilon'(t) + k \cdot \varepsilon(t)) \cdot sign(\varepsilon) > 0 \\ 0 \ at \ (T \cdot \varepsilon'(t) + k \cdot \varepsilon(t)) \cdot sign(\varepsilon) < 0 \end{cases} \tag{3}$$

$$\varepsilon^*(t) = \begin{cases} k \cdot \varepsilon(t) + T \cdot \varepsilon'(t) \ at \ \varepsilon'(t) \cdot \varepsilon''(t) \geq 0 \\ k \cdot \varepsilon(t) - T \cdot \varepsilon'(t) \ at \ (k \cdot \varepsilon(t) + T \cdot \varepsilon'(t)) \cdot \varepsilon'(t) < 0 \\ -k \cdot \varepsilon(t) + T \cdot \varepsilon'(t) \ at \ (k \cdot \varepsilon(t) + T \cdot \varepsilon'(t)) \cdot \varepsilon'(t) < 0 \end{cases} \tag{4}$$

A common feature of existing logic algorithms is that they analyze the controlled object functioning based on the regulation error function $\varepsilon(t)$ and its derivatives $\varepsilon'(t)$ and $\varepsilon''(t)$ discrete assessment. This approach helps maintain some insensitivity to changes in the object's parameters. However, these algorithms are designed for controlling a single controlled parameter and do not account for the interactions between separate subsystems, which is typical for MCACS in general and for helicopter TE specifically.

To address this issue, a dual-channel logic controller is proposed, which generates control actions for each separate subsystem while accounting for the cross-links impact on the output variables dynamics. This MCACS structure is shown in Figure 2, where $\mathbf{U}^*(t)$ represents the logically adjusted control coordinates vectors.

The proposed dual-channel logic controller operation, presented in Figure 3, is based on integrating a primary control algorithm for each separate subsystem. This algorithm adjusts the control error signal by analyzing both the current and predicted states. Additionally, a secondary logic algorithm creates artificial cross-links between subsystems to coordinate and the MCACS overall movement harmonize.
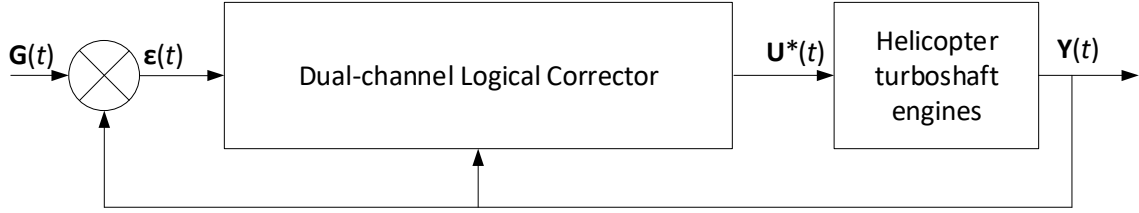
Figure 2: The helicopter turboshaft engines multi-connected automatic control system with a dual-channel logical controller structural diagram.
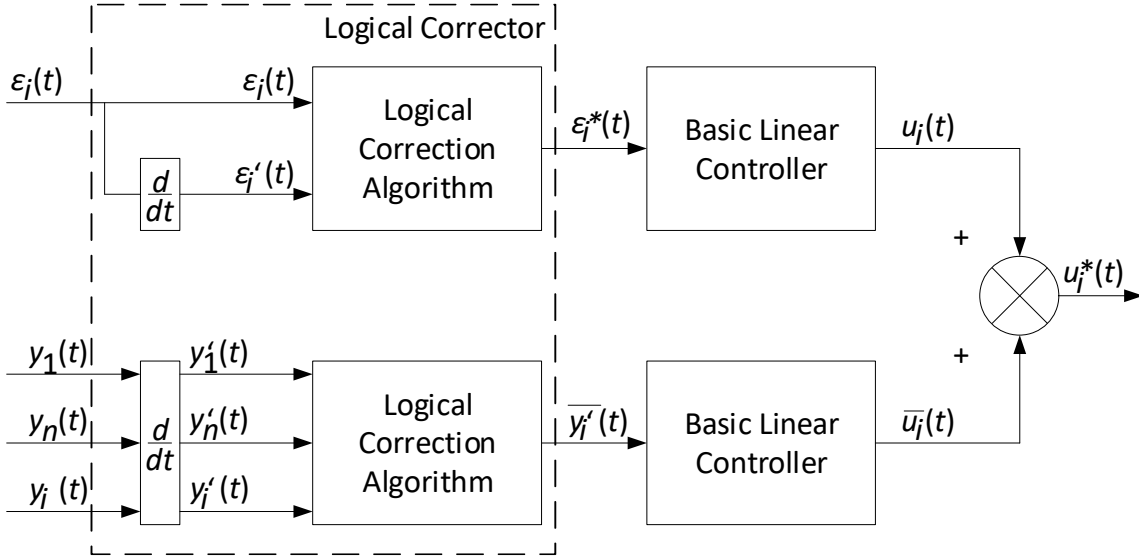
Figure 3: The two-channel logic controller for the *i*-th subsystem structural diagram.

The logic correction algorithm [38, 39] generates the primary logic error $\varepsilon_i^*(t)$ by discretely analyzing the current control error $\varepsilon_i(t)$ and its rate of change $\varepsilon_i'(t)$ for the *i*-th separate subsystem. The primary logic error includes dynamic changes to coefficients T_{log} and K_{log}, allowing the system to adapt to varying conditions:

$$\varepsilon_i^*(t) = \begin{cases} \varepsilon_i(t) \ at \ (\varepsilon_i(t) \cdot \varepsilon_i'(t) \leq 0) \wedge (\varepsilon_i(t) \cdot \varepsilon_i^{pred}(t) \geq 0) \\ \varepsilon_i(t) + T_{log} \cdot \varepsilon_i'(t) \ at \ (\varepsilon_i(t) \cdot \varepsilon_i'(t) \leq 0) \wedge (\varepsilon_i(t) \cdot \varepsilon_i^{pred}(t) < 0) \\ K_{log} \cdot \varepsilon_i(t) + T_{log} \cdot \varepsilon_i'(t) \ at \ (\varepsilon_i(t) \cdot \varepsilon_i'(t) > 0) \end{cases} \quad (5)$$

where T_{log} and K_{log} are the logical control algorithm parameters, $\varepsilon_i^{pred}(t)$ is the control error $\varepsilon_i^*(t)$ predicted value. Here, T_{log} and K_{log} adapt based on the following relation:

$$T_{log}(t) = T_{log}^0 + \beta \cdot |\varepsilon_i(t)|, K_{log}(t) = K_{log}^0 + \gamma \cdot |\varepsilon_i'(t)|, \quad (6)$$

where T_{log}^0 and K_{log}^0 are initial values, and β and γ are adaptive coefficients.

The predicted error value is also updated to include nonlinear effects, which can improve prediction accuracy under high oscillation conditions:

$$\varepsilon_i^{pred}(t) = K_{log} \cdot tanh(\varepsilon_i(t)) + T_{log} \cdot tanh(\varepsilon_i'(t)). \tag{7}$$

The use of the hyperbolic tangent function smooths out sharp changes, which is particularly useful in nonlinear dynamic systems.

The coordinating logic algorithm [40] establishes the coordinating signal $\bar{u}_i(t)$ based on the logic signal $\bar{y}_i'(t)$, which is derived from a comparative analysis of the dynamics $y_i'(t)$ of the i-th subsystem with the dynamics $y_j'(t)$ of the other j-th subsystems. The coordinating signal incorporates a nonlinear dependence on the parameter $\alpha_{log}(t)$, which adapts based on the mismatch in the subsystems dynamics:

$$\bar{y}_i'(t) = \begin{cases} 0 \; at \; (y_i'(t) \cdot y'(t) \geq 0) \wedge (y_i^{dev}(t) \leq 0) \\ -\alpha_{log} \cdot y'(t) \; at \; (y_i'(t) \cdot y'(t) \geq 0) \wedge (y_i^{dev}(t) > 0) \\ \alpha_{log} \cdot y'(t) \; at \; (y_i'(t) \cdot y'(t) < 0) \end{cases} \tag{8}$$

where α_{log} is the logical control algorithm parameter, $y'(t)$ is the leader dynamics among the j-th separate subsystems:

$$y'(t) = max\left(y_j'(t)\right), j = 1,2, \dots, n, j \neq i. \tag{9}$$

Here, $\alpha_{log}(t)$ also changes based on the deviation in the dynamics:

$$\alpha_{log}(t) = \alpha_{log}^0 + \delta \cdot \left|y_i^{dev}(t)\right|, \tag{10}$$

where δ is an adaptive coefficient.

The dynamics deviation of the i-th separate subsystem from the "leader" dynamics is determined according to the expression:

$$y_i^{dev}(t) = \left(y_i'(t) - y'(t)\right)^2 \cdot exp(-\lambda \cdot |y_i'(t) - y'(t)|), \tag{11}$$

where λ is a damping coefficient, reducing the large deviations impact.

The proposed dual-channel logical controller allows generating a control signal for MCACS each separate subsystem, taking into account the remaining subsystems influence. This enhanced model, featuring adaptive and nonlinear elements, provides more precise correction and coordination in control systems and is particularly useful in situations involving unpredictable changes in subsystem dynamics.

The key improvements in this model lie in the adaptive parameters T_{log}, K_{log} and α_{log} introduction which dynamically adjust based on system conditions, enhancing the control system responsiveness and stability. Nonlinear functions like tanh and exponential damping ensure smoother transitions, better handling of abrupt changes, and reduced oscillations, enhancing control precision. These improvements make the model more robust and effective in complex, nonlinear environments.

4. Results

This research addresses the evaluation of the effectiveness of the proposed dual-channel logic controller within the helicopter TE MCACS separate subsystems under flight parameter variations from test conditions (H = 0 km, V = 0 M). As a multi-input control object, the helicopter TE (with three regulated coordinates (n_{TC}, n_{FT}, T_G^*) and one control input (G_T), see Table 1 [41−43]) in test mode is described by the following transfer matrix function, considering the time constant T_{act} = 0.35 second for the aperiodic actuator [44]:

$$W_{reg}(s) = \frac{1}{0.25 \cdot s^2 + s + 1} \times$$

$$\times \begin{pmatrix} 0.5 & 0.6 & -0.2 \\ 0.2 \cdot (0.2 \cdot s + 1) & 0.65 \cdot (0.35 \cdot s + 1) & -0.15 \cdot (0.4 \cdot s + 1) \\ 0.75 \cdot (0.35 \cdot s + 1) & -0.65 \cdot (0.25 \cdot s + 1) & 0.2 \cdot (0.35 \cdot s + 1) \end{pmatrix}. \tag{12}$$

Table 1
The training dataset fragment [41–43]

Number	The gas-generator rotor r.p.m. n_{TC}	The gas temperature in front of the compressor turbine T_G^*	The free turbine rotor speed n_{FT}	The fuel consumption G_T
1	0.973	0.961	0.975	0.973
...	...	...	...	...
42	0.983	0.966	0.979	0.977
...	...	...	...	...
139	0.988	0.950	0.988	0.970
...	...	...	...	...
256	0.985	0.952	0.980	0.971

The training dataset homogeneity assessment, as described in [41–43], was conducted using the Fisher-Pearson [45] and Fisher-Snedecor [46] criteria. Based on these metrics, the dataset is considered homogeneous since the calculated Fisher-Pearson and Fisher-Snedecor values fall below their respective critical limits, specifically $\chi^2 = 5.984 < \chi^2_{critical} = 6.6$ and $F = 2.347 < F_{critical} = 2.58$. To assess dataset representativeness, a k-means cluster analysis [47, 48] was performed. The dataset was split into training and test subsets in a 2:1 ratio (67 and 33 %, or 172 and 84 samples, respectively). Cluster analysis (Table 1) identified eight distinct classes (I...VIII), confirming the presence of these groups and demonstrating consistency between the training and test subsets (Figure 4). These results helped determine the optimal sample sizes: the full training dataset consists of 256 elements, the validation dataset includes 172 elements (67 % of the training dataset), and the test dataset contains 84 elements (33 % of the training dataset).
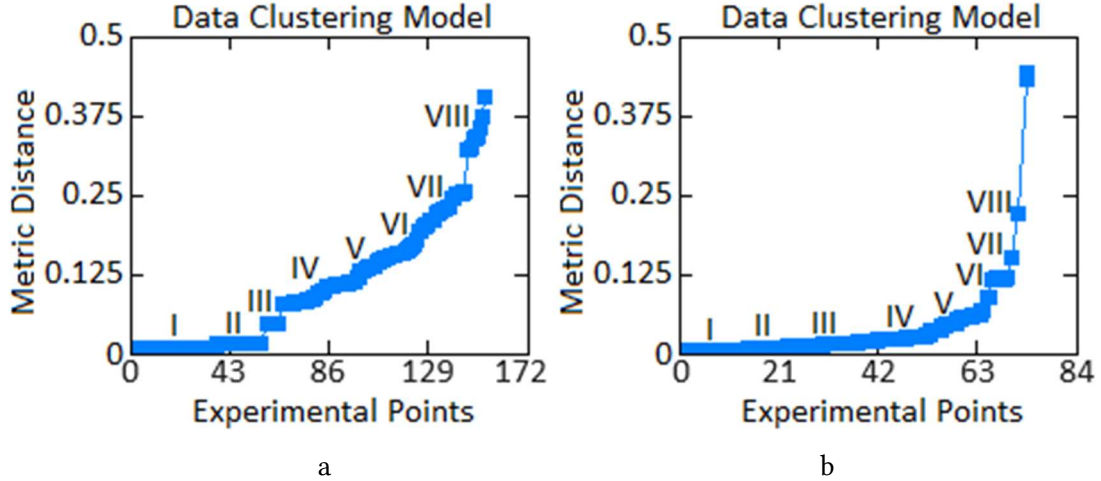
Figure 4: The cluster analysis results: a is the training dataset, b is the test dataset (author's research, published in [41–43]).

For the helicopter TE MCACS controlled parameters under bench conditions, according to [48], the following technical requirements for the performance characteristics are established: astatism of order V = 1, stabilization time t_{stab} < 5 seconds, no overshoot (σ = 0 %). Within these requirements framework, the main multidimensional linear controller parameters were calculated:

$$W_{reg}(s) = \frac{0.65 \cdot s + 1}{0.1 \cdot s + 1} \cdot \begin{pmatrix} 1.5 & 0 & 0 \\ 0 & 1.5 & 0 \\ 0 & 0 & 8.5 \end{pmatrix}. \tag{13}$$

The parameters for the logical corrector in each separate subsystem were calculated based on the conditions for coordination and stabilization of all output variables:

- Subsystem controlling the gas-generator rotor r.p.m. (n_{TC}): T_{log} = 0.6 second, K_{log} = 1, α_{log} = 0.2;
- Subsystem controlling the free turbine rotor speed (n_{FT}): T_{log} = 0.5 second, K_{log} = 2, α_{log} = 0.35;
- Subsystem controlling the gas temperature before the compressor turbine (T_G^*): T_{log} = 0.8 second, K_{log} = 4, α_{log} = 0.3.

According to the dual-channel logical controller configuration (Figure 3), the additional linear regulator within each i-th separate subsystem is described by the specified transfer function [49–51]:

$$G_i(s) = s^{-1}, i = 1,2,3. \tag{14}$$

The transition process diagrams for the output coordinate $\mathbf{Y}(t)$ in the analyzed helicopter engine control system (using the TV3-117 engine as an example) with the proposed two-channel logical controller are shown in Figure 5.
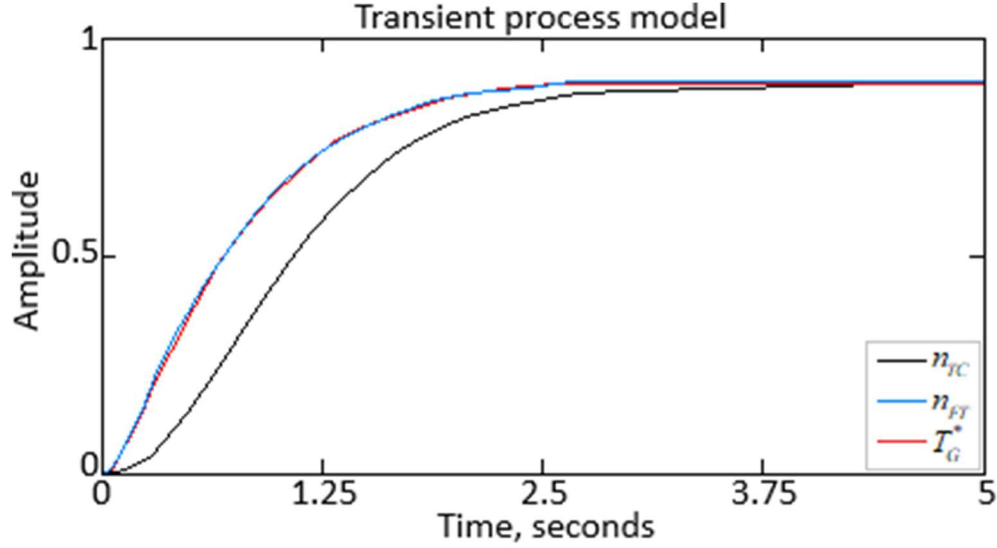
Figure 5: Diagrams of transient processes $\mathbf{Y}(t)$ in the TV3-117 engine studied multi-connected automatic control systems in the bench mode (author's research).

It is evident that the studied MCACS with the proposed dual-channel logical controllers ensures the desired performance for the TV3-117 engine control in the bench mode. This research examines the helicopter TE (using the TV3-117 engine as an example) two operating modes, corresponding to the following flight conditions:

- Point P_1 (H = 2.5 km, V = 0.68 Mach), where the helicopter TE (using the TV3-117 as an example) is represented by the following MTF:

$$\mathbf{W}_{TE}(s) = \frac{1}{0.42 \cdot s^2 + 1.34 \cdot s + 1} \times$$
$$\times \begin{pmatrix} \dfrac{0.72}{0.38 \cdot (0.39 \cdot s + 1)} & \dfrac{0.77}{0.63 \cdot (0.31 \cdot s + 1)} & \dfrac{-0.12}{-0.11 \cdot (0.48 \cdot s + 1)} \\ \dfrac{0.93 \cdot (0.57 \cdot s + 1)}{} & -0.74 \cdot (0.27 \cdot s + 1) & 0.14 \cdot (0.33 \cdot s + 1) \end{pmatrix}. \tag{15}$$

- Point P_2 (H = 4.2 km, V = 0.86 Mach), where the helicopter TE (using the TV3-117 as an example) is represented by the following MTF:

$$\mathbf{W}_{TE}(s) = \frac{1}{0.63 \cdot s^2 + 1.95 \cdot s + 1} \times$$
$$\times \begin{pmatrix} \dfrac{0.78}{0.42 \cdot (0.55 \cdot s + 1)} & \dfrac{0.91}{0.62 \cdot (0.35 \cdot s + 1)} & \dfrac{-0.24}{-0.12 \cdot (0.89 \cdot s + 1)} \\ 1.76 \cdot (0.88 \cdot s + 1) & -1.34 \cdot (0.32 \cdot s + 1) & 0.32 \cdot (0.68 \cdot s + 1) \end{pmatrix}. \tag{16}$$

The transition process diagrams for $\mathbf{Y}(t)$ in the TV3-117 engine studied MCACS, without the dual-channel logical controller, with a unit step input signal for each specified point P_{1-2}, are shown in Figures 6 and 7, respectively.
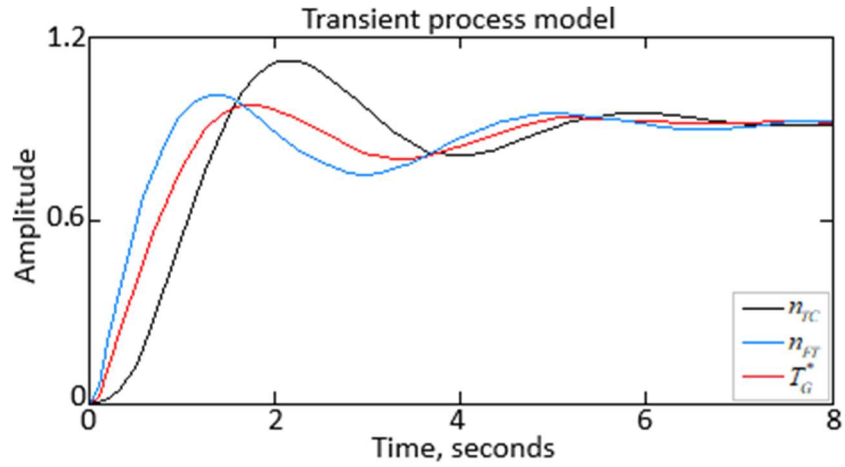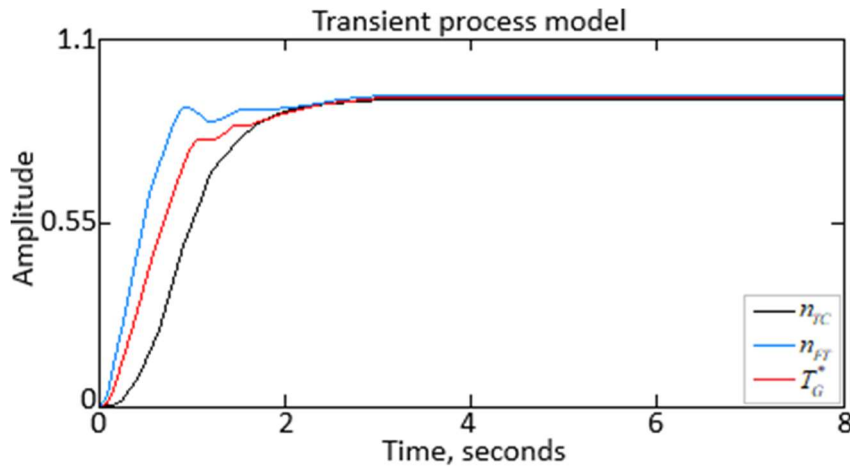
Figure 6: Diagrams of transient processes $\mathbf{Y}(t)$ in the TV3-117 engine studied multi-connected automatic control systems without logic controllers (point P_1) (author's research).
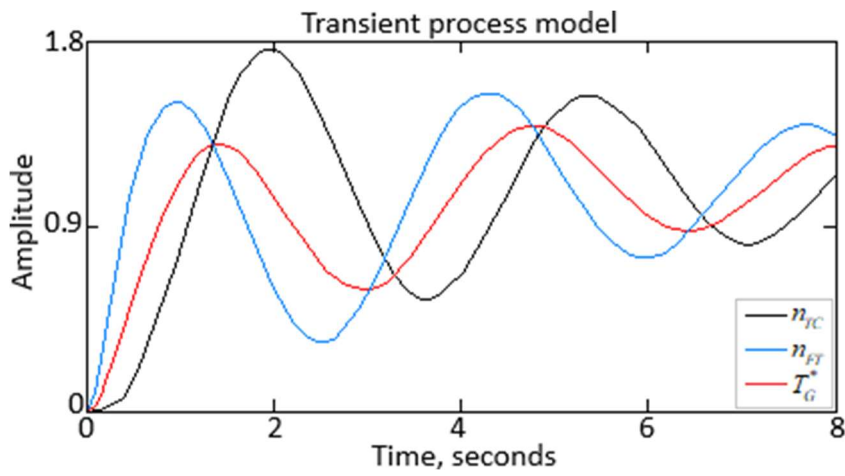
Figure 7: Diagrams of transient processes $\mathbf{Y}(t)$ in the TV3-117 engine studied multi-connected automatic control systems without logic controllers (point P_2) (author's research).

It is clear that the linear control algorithm fails to maintain the helicopter TE control quality when flight conditions change. However, the dual-channel logical controllers introduction significantly enhances the helicopter TE control quality with the control component remaining unchanged, as evidenced by Figures 8 and 9 for points P_1 and P_2, respectively.

Figure 8: Diagrams of transient processes $\mathbf{Y}(t)$ in the TV3-117 engine studied multi-connected automatic control systems with logic controllers (point P_1) (author's research).
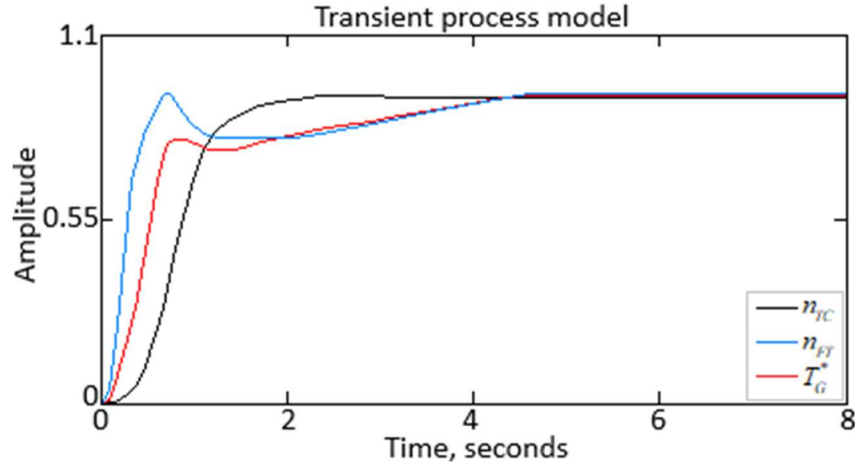
Figure 9: Diagrams of transient processes $\mathbf{Y}(t)$ in the TV3-117 engine studied multi-connected automatic control systems with logic controllers (point P_2) (author's research).

Thus, based on the helicopter TE MCACS computer simulation results (using the TV3-117 engine as an example), it is established that the proposed dual logical control algorithm significantly improves control quality across various flight modes.

5. Discussions

In this research, a dual-channel logic controller (see Figure 2) was synthesized, which generates control actions for each separate subsystem while considering the impact of cross-links on the output variables dynamics. The proposed dual-channel logic controller operation principle (see Figure 3) is based on integrating a primary logic control algorithm for the separate subsystem, which adjusts the error signal based on the current and predicted states analysis, and a secondary logic algorithm that creates artificial cross-links between subsystems to coordinate and harmonize the helicopter overall movement.

The research addresses the effectiveness evaluating task of the helicopter TE (using the TV3-117 engine as an example) proposed dual-channel logic controller within the separate subsystems under varying flight parameters compared to the bench test conditions (H = 0 km, V = 0 Mach) (see Figure 5), as well as in two flight scenarios: at H = 2.5 km, V = 0.68 Mach (see Figures 6 and 8) and at H = 4.2 km, V = 0.86 Mach (see Figures 7 and 9). The results obtained demonstrate that the synthesized dual-channel logic control algorithm enhances performance across different helicopter flight modes. The error at the transient process final stage is defined as:

$$E = |y_{final} - y_{ss}|, \tag{15}$$

where y_{final} is the output signal final value at the transient process end, y_{ss} is the output signal steady-state value.

Figure 10 shows the error at the transient process end calculating results ("blue columns" represents the dual-channel logic controller use, "red columns" indicates no dual-channel logic controller) for points P_1 (Figure 10a) and P_2 (Figure 10b). As seen from Figure 10, without the dual-channel logic controller, the error reaches 2.58 %, while with its application, the error decreases by nearly 40 % and does not exceed 1 %. This indicates a significant improvement in the transient process control quality when using the dual-channel logic controller, demonstrating its effectiveness in reducing error and enhancing system accuracy.

In this research, while the proposed dual-channel logic controller (see Figure 2) demonstrates improved control performance across various flight modes, certain limitations must be acknowledged. The controller effectiveness, evaluated under different flight conditions (H = 0 km, V = 0 Mach; H = 2.5 km, V = 0.68 Mach; and H = 4.2 km, V = 0.86 Mach), is based on the TV3-117 engine specific case and may not fully generalize to other engine models or more complex operational scenarios. Additionally, the improvements observed, such as a reduction in error from 2.58 to below

1 %, are contingent on the controller's implementation and may vary with changes in system dynamics, external disturbances, or unmodeled interactions.

a

b
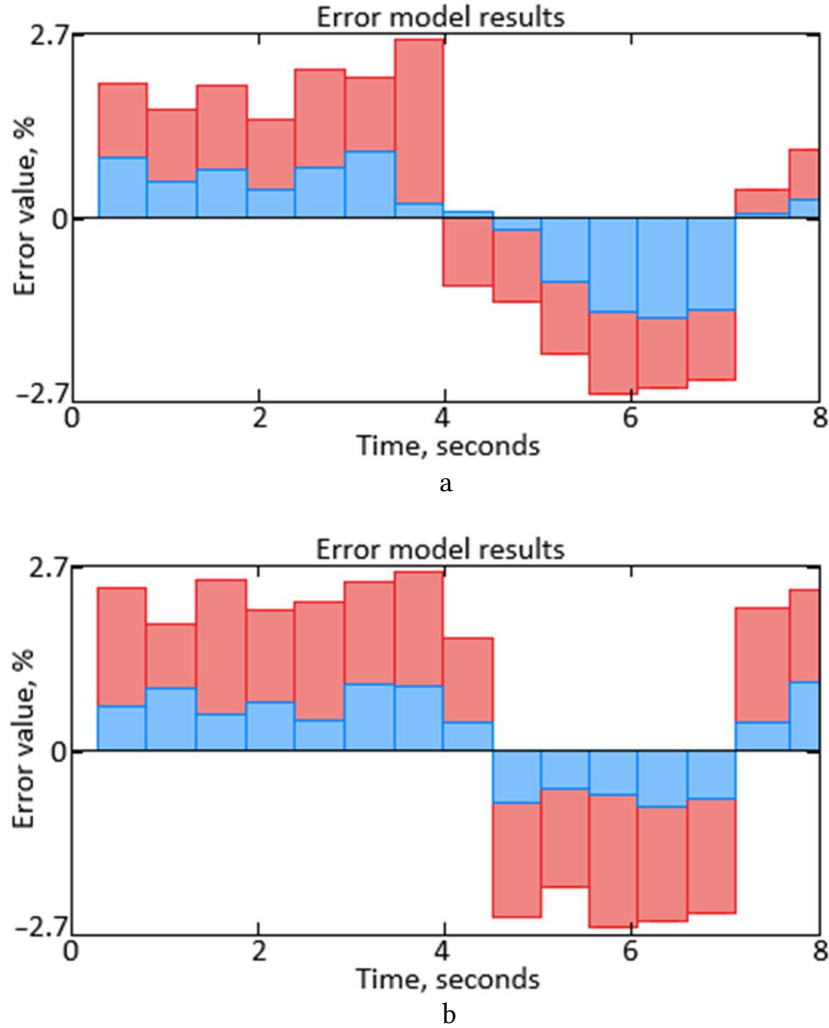
Figure 10: Diagrams of the error calculating results at the transient process final stage: a is the point P_1, b is the point P_2 (author's research).

The analysis presented in Figure 10 confirms significant enhancements in transient process control but does not account for potential limitations in robustness or scalability, which require further investigation to confirm the controller's effectiveness across a broader range of conditions and applications.

6. Conclusions

This research presents the proposed dual-channel logic controller within the helicopter turboshaft engines control systems evaluating results, demonstrating the effectiveness of this approach for controlling complex dynamic systems operating under conditions of parametric uncertainty. The developed dual logic algorithm stands out by considering not only the dynamics of output variables but also the influence of cross-links when generating control signals for each separate subsystem.

The research addresses the proposed dual-channel logic controller effectiveness assessing task within the helicopter turboshaft engines separate subsystems (using the TV3-117 engine as a case study) under varying flight parameters compared to bench test conditions (H = 0 km, V = 0 Mach), as well as in two flight scenarios: at H = 2.5 km, V = 0.68 Mach and at H = 4.2 km, V = 0.86 Mach. The results reveal that the synthesized dual logic control algorithm enhances performance across different helicopter flight modes.

It was found that the error at the end of the transient process, in the dual-channel logic controller absence, reaches 2.58 %, while with the controller's application, the error decreases by nearly 40 % and does not exceed 1 %. This indicates a substantial improvement in the transient process control quality with the dual-channel logic controller use.

Acknowledgements

References

[1]   M. Razmjooei, F. Ommi, Z. saboohi, Experimental analysis and modeling of gas turbine engine performance: Design point and off-design insights through system of equations solutions, Results in Engineering 23 (2024) 102495. doi: 10.1016/j.rineng.2024.102495.

[2]   X. Zheng, H. Zeng, B. Wang, M. Wen, H. Yang, and Z. Sun, Numerical simulation method of surge experiments on gas turbine engines, Chinese Journal of Aeronautics 36:3 (2023) 107–120. doi: 10.1016/j.cja.2022.08.007.

[3]   S. M. Hosseinimaab, A. M. Tousi, A new approach to off-design performance analysis of gas turbine engines and its application, Energy Conversion and Management 243 (2021) 114411. doi: 10.1016/j.enconman.2021.114411.

[4]   X. Liu, Y. Chen, L. Xiong, J. Wang, C. Luo, L. Zhang, K. Wang, Intelligent fault diagnosis methods toward gas turbine: A review, Chinese Journal of Aeronautics 37:4 (2024) 93–120, Apr. 2024. doi: 10.1016/j.cja.2023.09.024.

[5]   J. Song, Y. Wang, C. Ji, H. Zhang, Real-time optimization control of variable rotor speed based on Helicopter/ turboshaft engine on-board composite system, Energy 301 (2024) 131701. doi: 10.1016/j.energy.2024.131701.

[6]   S. Vladov, Y. Shmelov, R. Yakovliev, Helicopters Aircraft Engines Self-Organizing Neural Network Automatic Control System, CEUR Workshop Proceedings 3137 (2022) 28–47. doi: 10.32782/cmis/3137-3 URL: https://ceur-ws.org/Vol-3137/paper3.pdf

[7]   B. Jiang, K. Zhang, Y. Lu, Q. Miao, Fault Diagnosis and Fault-Tolerant Control of Helicopters, Reference Module in Materials Science and Materials Engineering. Elsevier, 2024. doi: 10.1016/b978-0-443-14081-5.00006-4.

[8]   H. Sheng, Q. Chen, J. Li, W. Jiang, Z. Wang, Z. Liu, T. Zhang, Y. Liu, Research on dynamic modeling and performance analysis of helicopter turboshaft engine's start-up process, Aerospace Science and Technology 106 (2020) 106097. doi: 10.1016/j.ast.2020.106097.

[9]   K. Yan, H. Chen, C. Chen, S. Gao, J. Sun, Time-varying gain extended state observer-based adaptive optimal control for disturbed unmanned helicopter, ISA Transactions 148 (2024) 1–11. doi: 10.1016/j.isatra.2024.02.028.

[10] C. Zhang, V. Gümmer, Multi-objective optimization and system evaluation of recuperated helicopter turboshaft engines, Energy 191 (2020) 116477. doi: 10.1016/j.energy.2019.116477.

[11] Y. Wang, Q. Zheng, Z. Xu, H. Zhang, A novel control method for turboshaft engine with variable rotor speed based on the Ngdot estimator through LQG/LTR and rotor predicted torque feedforward, Chinese Journal of Aeronautics 33:7 (2020) 1867–1876. doi: 10.1016/j.cja.2020.01.009.

[12] L. Chen, F. Hao, Optimal tracking control for unknown nonlinear systems with uncertain input saturation: A dynamic event-triggered ADP algorithm, Neurocomputing 564 (2024) 126964. doi: 10.1016/j.neucom.2023.126964.

[13] J. Xiao, Y. Liu, Y. An, Adaptive dynamic event-triggered fault tolerant control for uncertain strict-feedback nonlinear systems, European Journal of Control 79 (2024) 101096. doi: 10.1016/j.ejcon.2024.101096.

[14] X. Mao, Y. Xiang, J. Lu, An efficient nonlinear adaptive filter algorithm based on the rectified linear unit, Digital Signal Processing 146 (2024) 104373. doi: 10.1016/j.dsp.2023.104373.

[15] R. Kumar, Recurrent context layered radial basis function neural network for the identification of nonlinear dynamical systems, Neurocomputing 580 (2024) 127524. doi: 10.1016/j.neucom.2024.127524.

[16] T. V. Pham, Q. T. T. Nguyen, Adaptive formation control of nonlinear multi-agent systems with dynamic event-triggered communication, Systems & Control Letters 181 (2023) 105652. doi: 10.1016/j.sysconle.2023.105652.

[17] X. Ji, X. Zhang, S. Zhu, F. Deng, B. Zhu, Data-driven adaptive consensus control for heterogeneous nonlinear Multi-Agent Systems using online reinforcement learning, Neurocomputing 596 (2024) 127818. doi: 10.1016/j.neucom.2024.127818.

[18] J. Wang, Y. Wu, C. L. P. Chen, Z. Liu, W. Wu, Adaptive PI event-triggered control for MIMO nonlinear systems with input delay, Information Sciences 677 (2024) 120817. doi: 10.1016/j.ins.2024.120817.

[19] T. Li, L. Long, C. Huang, Supervisory adaptive safety control for uncertain nonlinear systems, Journal of the Franklin Institute 361:9 (2024) 106882. doi: 10.1016/j.jfranklin.2024.106882.

[20] S. Vladov, Y. Shmelov, R. Yakovliev, M. Petchenko, S. Drozdova, Neural Network Method for Helicopters Turboshaft Engines Working Process Parameters Identification at Flight Modes. In Proceedings of the 2022 IEEE 4th International Conference on Modern Electrical and Energy System (MEES), Kremenchuk, Ukraine, October 20–22, 2022, pp. 604–609. doi: 10.1109/MEES58014.2022.10005670.

[21] S. Vladov, R. Yakovliev, O. Hubachov, J. Rud, Neuro-Fuzzy System for Detection Fuel Consumption of Helicopters Turboshaft Engines, CEUR Workshop Proceedings 3628 (2024) 55–72. URL: https://ceur-ws.org/Vol-3628/paper5.pdf

[22] Y. Wang, A. Li, S. Yang, H. Tian, A model reference adaptive control scheme of a high-order nonlinear helicopter subject to input and state constraints, Journal of the Franklin Institute 359:13 (2022) 6709–6734. doi: 10.1016/j.jfranklin.2022.07.011.

[23] Z. Gu, Q. Li, S. Pang, W. Zhou, J. Wu, C. Zhang, Turbo-shaft engine adaptive neural network control based on nonlinear state space equation, Chinese Journal of Aeronautics 37:4 (2024) 493–507. doi: 10.1016/j.cja.2023.08.012.

[24] P. Kurdel, A. Novák, A. N. Sedláčková, L. Korba, The Methods of Helicopter Control in Non-standard Situations, Transportation Research Procedia 59 (2021) 214–222. doi: 10.1016/j.trpro.2021.11.113.

[25] R. M. Catana, G. Dediu, Analytical Calculation Model of the TV3-117 Turboshaft Working Regimes Based on Experimental Data, Applied Sciences 13:19 (2023) 10720. doi: 10.3390/app131910720.

[26] L. Gebrehiwet, Y. Nigussei, T. Teklehaynanot, A Review-Differentiating TV2 and TV3 Series Turbo Shaft Engines, International Journal of Research Publication and Reviews 3(8) (2022) 1822–1839. doi: 10.55248/gengpi.2022.3.8.55.

[27] S. Vladov, L. Scislo, V. Sokurenko, O. Muzychuk, V. Vysotska, S. Osadchy, A. Sachenko, Neural Network Signal Integration from Thermogas-Dynamic Parameter Sensors for Helicopters Turboshaft Engines at Flight Operation Conditions, Sensors 24:13 (2024) 4246. doi: 10.3390/s24134246.

[28] G. Ghazi, B. Gerardin, M. Gelhaye, R. M. Botez, New Adaptive Algorithm Development for Monitoring Aircraft Performance and Improving Flight Management System Predictions, Journal of Aerospace Information Systems 17:2 (2020) 97–112. doi: 10.2514/1.i010748.

[29] M. Montazeri-Gh, S. Abyaneh, Real-time simulation of a turbo-shaft engine's electronic control unit, Mechanics & Industry 18:5 (2017) 503. doi: 10.1051/meca/2017025.

[30] T. Castiglione, D. Perrone, L. Strafella, A. Ficarella, S. Bova, Linear Model of a Turboshaft Aero-Engine Including Components Degradation for Control-Oriented Applications, Energies 16:6 (2023) 2634. doi: 10.3390/en16062634.

[31] N. Gu, X. Wang, M. Zhu, Multi-Parameter Quadratic Programming Explicit Model Predictive Based Real Time Turboshaft Engine Control, Energies 14:17 (2021) 5539. doi: 10.3390/en14175539.

[32] I. M. A. Ibrahem, O. Akhrif, H. Moustapha, M. Staniszewski, Nonlinear generalized predictive controller based on ensemble of NARX models for industrial gas turbine engine, Energy 230 (2021) 120700. doi: 10.1016/j.energy.2021.120700.

[33] X. Liu, E. Song, L. Zhang, Y. Luan, J. Wang, C. Luo, L. Xiong, Q. Pan, Design and implementation for the state time-delay and input saturation compensator of gas turbine aero-engine control system, Energy 288 (2024) 129934. doi: 10.1016/j.energy.2023.129934.

[34] O. S. Gurevich, F. D. Golberg, S. A. Smetanin, M. E. Trifonov, Optimization of gas turbine aircraft engine control throughout the engine service life, Aerospace and Mechanical Engineering 17:4 (2018) 47–56. doi: 10.18287/2541-7533-2018-17-4-47-56.

[35] J. Liu, L. Wang, A. Yerudkar, Y. Liu, Set stabilization of logical control networks: A minimum node control approach, Neural Networks 174 (2024) 106266. doi: 10.1016/j.neunet.2024.106266.

[36] R. Zhou, Y. Guo, Y. Wang, Z. Sun, X. Liu, Safe control of logical control networks with random impulses, Neural Networks 165 (2023) 884–895. doi: 10.1016/j.neunet.2023.06.035.

[37] L. Wu, J. Sun, Optimal preview pinning control of Boolean networks, ISA Transactions 146 (2024) 291–296. doi: 10.1016/j.isatra.2023.12.029.

[38] Y. Li, H. Li, Y. Li, Constrained set controllability of logical control networks with state constraints and its applications, Applied Mathematics and Computation 405 (2021) 126259. doi: 10.1016/j.amc.2021.126259.

[39] H. Li, W. Dou, On reducible state variables of logical control networks, Systems & Control Letters 145 (2020) 104798. doi: 10.1016/j.sysconle.2020.104798.

[40] T. Sun, R. Wang, X. Zhao, P. Sun, Partial and Global Stabilization at An Attractor for k-valued Logical Control Networks, Journal of the Franklin Institute 357:11 (2020) 7003–7019. doi: 10.1016/j.jfranklin.2020.04.054.

[41] S. Vladov, R. Yakovliev, V. Vysotska, M. Nazarkevych, V. Lytvyn, The Method of Restoring Lost Information from Sensors Based on Auto-Associative Neural Networks, Applied System Innovation 7:3 (2024) 53. doi: 10.3390/asi7030053.

[42] S. Vladov, R. Yakovliev, M. Bulakh, V. Vysotska, Neural Network Approximation of Helicopter Turboshaft Engine Parameters for Improved Efficiency, Energies 17:9 (2024) 2233. doi: 10.3390/en17092233.

[43] S. Vladov, Y. Shmelov, R. Yakovliev, Method for Forecasting of Helicopters Aircraft Engines Technical State in Flight Modes Using Neural Networks, CEUR Workshop Proceedings 3171 (2022) 974–985. URL: https://ceur-ws.org/Vol-3171/paper70.pdf

[44] F. Ferrante, S. Tarbouriech, Sampled-data feedback control design in the presence of quantized actuators, Nonlinear Analysis: Hybrid Systems 54 (2024) 101530. doi: 10.1016/j.nahs.2024.101530.

[45] H.-Y. Kim, Statistical notes for clinical researchers: Chi-squared test and Fisher's exact test, Restorative Dentistry & Endodontics 42:2 (2017) 152. doi: 10.5395/rde.2017.42.2.152.

[46] C. M. Stefanovic, A. G. Armada, X. Costa-Perez, Second Order Statistics of Fisher-Snedecor Distribution and Their Application to Burst Error Rate Analysis of Multi-Hop Communications, IEEE Open Journal of the Communications Society 3 (2022) 2407–2424. doi: 10.1109/ojcoms.2022.3224835.

[47] Z. Hu, E. Kashyap, O.K. Tyshchenko, GEOCLUS: A Fuzzy-Based Learning Algorithm for Clustering Expression Datasets. Lecture Notes on Data Engineering and Communications Technologies 134 (2022) 337–349. doi: 10.1007/978-3-031-04812-8_29.

[48] S. Babichev, J. Krejci, J. Bicanek, V. Lytvynenko, Gene expression sequences clustering based on the internal and external clustering quality criteria. In Proceedings of the 2017 12th International

Scientific and Technical Conference on Computer Sciences and Information Technologies (CSIT), Lviv, Ukraine, 05–08 September 2017. doi: 10.1109/STC-CSIT.2017.8098744.

[49] Z. Hu, I. Dychka, K. Potapova, V. Meliukh, Augmenting Sentiment Analysis Prediction in Binary Text Classification through Advanced Natural Language Processing Models and Classifiers, International Journal of Information Technology and Computer Science 16:2 (2024) 16–31. doi: 10.5815/ijitcs.2024.02.02.

[50] E. M. Cherrat, R. Alaoui, H. Bouzahir, Score fusion of finger vein and face for human recognition based on convolutional neural network model, International Journal of Computing 19:1 (2020) 11–19. doi: 10.47839/ijc.19.1.1688.

[51] B. Rusyn, O. Lutsyk, R. Kosarevych, O. Kapshii, O. Karpin, T. Maksymyuk, J. Gazda, Rethinking Deep CNN Training: A Novel Approach for Quality-Aware Dataset Optimization, IEEE Access 12 (2024) 137427–137438. doi: 10.1109/access.2024.3414651.